Kinetics of H_2 desorption from crystalline C_{60}

S. A. FitzGerald,[1] R. Hannachi,[1] D. Sethna,[1] M. Rinkoski,[1] K. K. Sieber,[2] and David S. Sholl[2,3]
[1]*Oberlin College, Department of Physics, Oberlin, Ohio 44074, USA*
[2]*Department of Chemical Engineering, Carnegie Mellon University, Pittsburgh, Pennsylvania 15213, USA*
[3]*National Energy Technology Laboratory, Pittsburgh, Pennsylvania 15236, USA*
(Received 27 July 2004; revised manuscript received 30 September 2004; published 13 January 2005)

The nonequilibrium diffusion of H_2 within crystalline C_{60} is examined by monitoring the outgassing of H_2 from C_{60} powders. Results show that the desorption-lifetime decreases dramatically with increasing H_2 concentration. Kinetic Monte Carlo simulations indicate that diffusion occurs by H_2 molecules hopping between interstitial octahedral sites via an energetically unstable intermediary tetrahedral site. This diffusion is greatly enhanced by the presence of dimers in which two H_2 molecules briefly occupy the same octahedral site. The abundance of dimers increases with H_2 concentration and leads to simulated desorption curves that are in good agreement with the experimental outgassing data.

DOI: 10.1103/PhysRevB.71.045415 PACS number(s): 78.30.Na, 66.30.Jt, 82.20.Kh

INTRODUCTION

There is presently much interest in the storage and transport of hydrogen within novel forms of carbon. Most of the work on this topic has focused on carbon nanotubes and the desire to achieve large loading concentrations of hydrogen.[1–3] However, macroscopic quantities of carbon nanotubes tend to be highly inhomogeneous with large numbers of defects and impurities. As such it is very difficult to obtain clean experimental data to unambiguously compare with theoretical models of the carbon hydrogen interactions.

In contrast, solid C_{60} (fullerite) can be easily obtained as a highly crystalline well-characterized material. Above $T=260$ K C_{60} forms an fcc lattice in which the C_{60} molecules are freely rotating.[4] For each C_{60} the lattice has one large interstitial void (radius $\sim$2.1 Å) with octahedral (O) symmetry and two somewhat smaller voids (radius $\sim$1.1 Å) with tetrahedral (T) symmetry.[5] It is now known that weak van der Waals–type forces can reversibly trap molecular hydrogen[6] and other small atoms and molecules such as He, Ne, Ar, Kr, Xe, O_2, N_2, CO, and CO_2, within the O sites of C_{60}.[7–11]

The mechanisms by which adsorbed hydrogen molecules diffuse within the C_{60} lattice are still not fully understood. Geometric considerations suggest that H_2 molecules diffuse within the lattice by a hopping mechanism in which the H_2 jumps from O site to O site via the energetically unstable T site. The rate-limiting step occurs when the H_2 hops out of an O site over the barrier into the T site. Uberuaga *et al.* recently proposed that this diffusion process is greatly enhanced by the presence of short-lived dimers in which two H_2 occupy the same O site.[12] Essentially, the presence of the first H_2 in an O site raises the energy of a second H_2 (through H_2—H_2 repulsion) and thus reduces the energy required to hop out of the O site. Uberuaga *et al.* modeled the impact of this process on the concentration dependent self diffusivity of H_2 in C_{60}, $D_s(c)$, and predicted that this quantity increases as the H_2 concentration is increased.

In this paper we examine the diffusion mechanism proposed by Uberuaga *et al.* by directly comparing our experimental and computer simulation data for the desorption kinetics of H_2 from C_{60} crystallites. The experimental results are obtained by monitoring the H_2 outgassing through a simple pressure increase within a cell of known volume. The theoretical calculations, presented in the analysis section, use kinetic Monte Carlo (KMC) simulations of the lattice model developed by Uberuaga *et al.*[12] to derive diffusion coefficients suitable for describing macroscopic mass transfer through C_{60} crystallites.

In anticipation of our results, it is useful to consider how the desorption kinetics from a C_{60} particle would occur if the dimer diffusion mechanism described above played no role in H_2 diffusion. In this case, it would be reasonable to describe H_2 diffusion as a series of single-particle hops between O sites (moving via metastable T sites), where the only role of H_2—H_2 interactions is to prohibit H_2 molecules from entering an already occupied O site. The diffusion properties of species diffusing on a lattice of sites with simple site blocking of this type is well known; the self-diffusion coefficient decreases monotonically with increasing concentration, while the transport diffusivity is independent of concentration.[13,14] The transport diffusivity $D_T(c)$, is the quantity that relates the flux of a diffusing species $\vec{J}$ to a gradient in the concentration of that species via Fick's law $\vec{J}=-D_T(c)\nabla c$. When the transport diffusivity is independent of concentration, Fick's law for the desorption of gas from a spherical grain of radius R can be solved in closed form, giving[15]

$$\overline{c}(t)/c_0 = \frac{6}{\pi^2}\sum_{j=1}^{\infty}\frac{1}{j^2}\exp\left(-\frac{j^2\pi^2 D_t t}{R^2}\right). \quad (1)$$

Here $\overline{c}(t)$ is the average adsorbate concentration within the grain at time t and c_0 the initial concentration, which is assumed to be uniform throughout the grain. The key observation to be made from this expression is that any reasonable definition of the characteristic time describing desorption is independent of the initial concentration.

One of the main predictions of the dimer diffusion mechanism proposed by Uberuaga *et al.* is that the diffusion coefficients of H_2 will deviate strongly from the simpler model outlined above. Below, we explore the implications of this mechanism for desorption processes similar to those described above and compare the results of this analysis with experimental measurements.

EXPERIMENTAL PROCEDURE

The C_{60} powder obtained commercially from MER Corporation was initially sieved to obtain a more uniform particle size distribution. Scanning electron microscope measurements indicated an average particle size of 50 μm with a standard deviation of 10 μm. The powder was heated under vacuum at 450 K for two days to remove any residual solvent. 0.6 g of powder were placed inside the sample cell and evacuated *in situ* at elevated temperature to remove any adsorbed gases immediately before loading with hydrogen. The loading pressure (on the order of 100–300 bar) was maintained for more than 24 h to assure equilibrium conditions had been achieved.

The desorption process was initiated by rapidly evacuating (on the order of 10 s) the sample cell to a base pressure of less than 0.1 mbar. The subsequent outgassing of the sample was monitored by the pressure increase within the cell of known volume (10 cm^3) over the course of some 4–8 h. A typically final outgas pressure was on the order of 0.5 bar. Control measurements on a blank cell produced negligible outgassing relative to that of the sample. The system was maintained at 273 K throughout the experiment by placing it in an ice bath.

Calibration of the initial concentration of adsorbed H_2 as a function of loading pressure was obtained using the method outlined in previous papers.[6,16] The system was loaded under the same conditions (pressure, temperature) as the degassing runs. Once loaded the sample cell was rapidly quenched in liquid nitrogen, kinetically trapping all the adsorbed H_2 within the C_{60} lattice. The system was then evacuated and the cell warmed back to room temperature, which degasses essentially all of the adsorbed H_2 into the calibrated volume. Knowledge of the final pressure increase and mass of C_{60} allowed us to determine the initial H_2 concentration.

EXPERIMENTAL RESULTS

Figure 1 shows a typical outgassing curve. There is a rapid initial outgas within the first few minutes followed by a much slower tail that persists for more than an hour. The curve is clearly quite different from a simple exponential behavior. Similar trends have been reported for both Ne and O_2 outgassing from C_{60}.[17–19] We also ran tests on a finely ground C_{60} powder and a collection of large single crystals (few mm in diameter). In both cases the shape of the outgassing curves were quite similar to those shown in Fig. 1, but the time scales were significantly different varying from a few minutes to several days. These observations are consistent with diffusion within the C_{60} grains being the rate-determining step for mass transfer in these experiments.

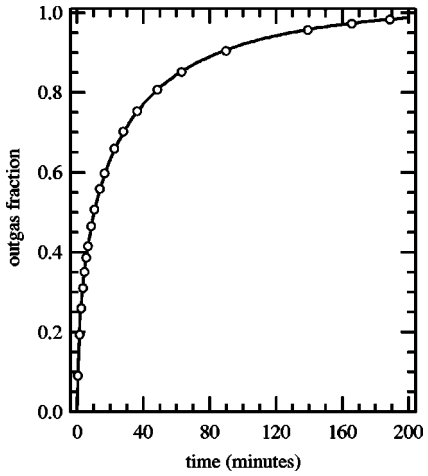

FIG. 1. A typical outgassing curve obtained on a C_{60} powder with mean particle size of 50 μm. The data are fit to a stretched exponential function.

Figure 2 shows normalized outgassing curves for three different initial H_2 loading concentrations. Pressure constraints limited us to loading configurations with at most 60% of the *O* sites initially occupied. The data indicate that the time scale for outgassing decreases significantly with increasing initial hydrogen concentration.

The outgassing curves in Fig. 2 and similar experiments at other initial concentrations are not consistent with the simple exponential form of Eq. (1). This observation by itself does not prove that Eq. (1) is physically incorrect, since the outgassing curves arise from desorption by a large number of individual C_{60} grains packed in a complex (and unknown) manner. If diffusion within the C_{60} grains is rate limiting, however, the observation that the characteristic time associated with desorption in Eq. (1) is independent of the initial

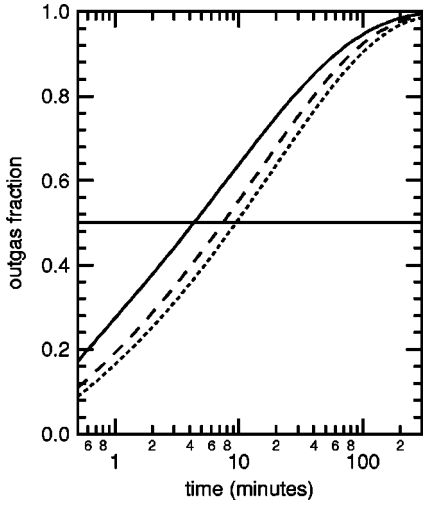

FIG. 2. Outgassing curves for three different initial H_2 concentrations. Solid line shows results for an initial fill fraction of 0.6, dashed line 0.4, and dotted line 0.16. The data are shown on a semilog plot for clarity in distinguishing between the different curves at early times. The line at 0.5 outgassing is provided as a guide for the eye. All data were taken at 273 K.

TABLE I. Fitting parameters of experimental outgassing curves for different initial loading concentration.

Initial H_2 fill fraction	τ (min)	β
0.09	19.2	0.49
0.16	17.8	0.49
0.28	16.6	0.49
0.37	13.5	0.47
0.44	10.5	0.44
0.54	9.1	0.42
0.61	7.7	0.42

concentration is also correct for arbitrary spatial arrangements of grains. That is, if the simple model underlying Eq. (1) is correct, we would expect to see a more complex desorption profile than a simple exponential from a realistic experiment with many grains, but the functional form of the normalized desorption rate would still be independent of the initial concentration.

To analyze our experimental data further, it is useful to define the characteristic time associated with desorption from a given initial concentration. We found that each outgassing profile could be fitted effectively using a stretched exponential form

$$P(t) = P_f(1 - \exp[-(t/\tau)^{\beta}]), \tag{2}$$

where P_f is the final pressure, τ the time constant, and the stretching exponent β can vary between 0 and 1. Stretched exponential behavior has been shown to model a wide range of relaxation phenomena and in the case of diffusion has traditionally been applied to jump diffusion within glasses containing random potential barriers between different sites.[20] Our intent here is to treat this stretched exponential dependence as a phenomenological model that provides a convenient method for quantifying our outgassing curves. The fitting parameters summarized in Table I show a strong decrease in time constant τ with initial concentration. A much weaker concentration dependence is observed for the stretching exponent β.

To ensure that the observed concentration dependence in τ was not simply an artifact of our fitting procedure we also examined the "half-life" defined as the time for the outgassing pressure to reach half of its final value. The guide line in Fig. 2 makes it easy to determine this value and one can see that there is again a decrease of more than a factor of 2 in the lifetime over the concentration range studied.

THEORETICAL MODELING

In this section, we describe calculations that allow us to compare the diffusion that occurs by the dimer mechanism proposed by Uberuaga *et al.*[12] with our outgassing experiments. A lattice model was derived by Uberuaga *et al.* to describe the interstitial diffusion of H_2 among the *O* and *T* sites of C_{60} using activation energies calculated from atomically detailed simulations. The largest activation barrier is associated with the step in which an H_2 molecule hops out of the *O* site and into the energetically unstable *T* site. However, the simulations revealed that this barrier could be significantly reduced by the existence of metastable states in which two H_2 molecules reside in a single *O* site. The lattice model accounts for the energies and hopping rates associated with both these dimer states and the much less stable trimers that can also form.[12] The model of Uberuaga *et al.* does not account for zero-point corrections to the energies of adsorbed molecules. It is likely that inclusion of these effects would not cause significant corrections to the energy barriers associated with the various H_2 hopping events.

Uberuaga *et al.* previously used their lattice model to predict the self-diffusion coefficient $D_s(c)$ for H_2 in C_{60} as a function of temperature and concentration. The self-diffusion coefficient measures the mobility of a single tagged molecule.[21–23] These calculations showed that the existence of H_2 dimers leads to a self diffusivity that increases rapidly with increasing interstitial H_2 concentration.[12] The temperature dependence of the self diffusivity was also found to be quite weak near room temperature.

In order to model the desorption of H_2 from C_{60} particles as observed in our experiments, it is necessary to calculate the transport diffusivity $D_T(c)$, which as already stated, relates the resultant macroscopic flux $\vec{J}$ to a concentration gradient via Fick's law $\vec{J} = -D_T(c)\nabla_c$. Transport diffusivities can be computed from either lattice or off-lattice models using either nonequilibrium or equilibrium simulations.[13,14,24–27] We used KMC simulations of the lattice model of Uberuaga *et al.* to examine the motion of ensembles of H_2 molecules within a C_{60} crystal at equilibrium. Numerical tests were performed to be sure that our computational domains were large enough to avoid any finite-size effects. As shown in previous studies of molecular diffusion in zeolites, appropriate analysis of equilibrium simulations allows the concentration-dependent transport diffusivity to be determined.[25,26] In particular, our KMC simulations were analyzed to determine the so-called corrected diffusivity $D_0(c)$ as a function of concentration.[13,21,22,27] The results can be fit to a simple phenomenological model

$$\frac{D_0(c)}{D(0)} = (A + Bc)^D, \tag{3}$$

where the parameters $A = 1.04$, $B = -1.007$, and $D = -1.07$ are all close to 1 and $D(0)$ is the diffusion coefficient of an isolated H_2 molecule in C_{60}. The concentration is written in units, where $c = 1$ corresponds to one H_2 molecule per C_{60} O site. The corrected diffusivity is a monotonically increasing function of c, similar to the self-diffusivity.[12] We note that in the limit $c \to 0$ the self-diffusion, corrected diffusion, and transport diffusion coefficients must all be equal, so there is no ambiguity in referring to $D(0)$ as simply the diffusion coefficient of an isolated interstitial molecule.

The value of computing the corrected diffusivity is that it is rigorously related to the transport diffusivity D_T by[21–23]

$$\frac{D_T(c)}{D(0)} = \frac{D_0(c)}{D(0)} \frac{\partial \ln f}{\partial \ln c}, \tag{4}$$

where f is the fugacity of the gas phase H_2 in equilibrium with the interstitial H_2 at concentration c and the derivative

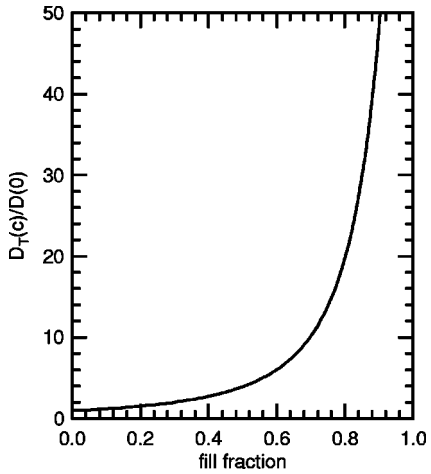

FIG. 3. Transport diffusivity for H_2 in C_{60} obtained through KMC simulations as described in Eqs. (3)–(5) in the text.

term is known as the thermodynamic correction factor.[21–23] Several methods are available to calculate the thermodynamic correction factor for lattice models. We used the method of Uebing and Gomer,[26] where the equilibrium interstitial concentration corresponding to a specified gas phase chemical potential is determined using grand canonical Monte Carlo (GCMC) and the thermodynamic correction factor for that concentration is defined by the fluctuations about the average concentration in the simulations. The chemical potential in our GCMC simulation was related to the fugacity by treating the gas phase as ideal. Fitting the resulting data at 300 K gave

$$\frac{\partial \ln f}{\partial \ln c} = (A_1 + A_2 c)/(1 + A_3 c + A_4 c^2), \tag{5}$$

with $A_1 = 1.0$, $A_2 = -0.7738$, $A_3 = -1.8200$, and $A_4 = 0.85255$. This functional form correctly captures the fact that the thermodynamic correction factor becomes unity in the limit of low concentrations. Our GCMC simulations show that the adsorption isotherm predicted by our lattice model is well described by a Langmuir isotherm for $c < 0.8$, in excellent agreement with experimental observations.[16] For higher concentrations, which were not probed in the experimental isotherm reported in Ref. 16 or in the experiments reported here, deviations from the Langmuir form become apparent.

Using Eqs. (3) and (5) in Eq. (4) defines the concentration-dependent transport diffusivity shown in Fig. 3. Similar to the self-diffusivity, the transport diffusivity increases as the interstitial concentration is increased. This is in striking contrast to behavior obtained from the lattice model if dimers and trimers are excluded. In this case we get the simple noninteracting lattice gas discussed in the introduction, which has a transport diffusivity independent of concentration.[14]

The purpose of determining the Fickian diffusivity from our lattice model is to allow us to examine numerically the desorption kinetics of H_2 from crystalline C_{60}. We used the diffusion coefficient described above to model the macroscopic desorption of H_2 from spherical pellets of radius R filled with a uniform initial concentration c_0. Several particle radii were simulated, establishing that the results reported below are essentially independent of the particle radius. We assumed that desorption of H_2 from the surface of C_{60} was not rate limiting, so the evolution of the H_2 concentration in a pellet can be written as

$$\frac{\partial c}{\partial t} = -\nabla [D_T(c) \nabla c] \quad \text{for } 0 \leqslant r < R, \tag{6}$$

with $c(r,0) = c_0$ for $0 \leqslant r < R$. We also assumed that the gas phase pressure was negligible at all times during the experiment, so $c(R,t) = 0$ for $t > 0$. The same assumptions underlie the derivation of Eq. (1). We integrated Eq. (6) numerically using FEMLAB, a commercial finite element method code[28] to determine $\overline{c}(t)$, the average concentration remaining in the pellet at time t. To compare with the experimental method, we then fit the observed desorption profile to a stretched exponential, in the form of Eq. (2). The results of this fitting procedure for initial fill fractions varying from 0.1 to 0.9 H_2 per interstitial O site are summarized in Table II.

TABLE II. Fitting parameters of simulated outgassing curves for different initial loading concentration.

Initial H_2 fill fraction	τ (arbitrary)	β
0.1	1.0	0.70
0.2	0.95	0.69
0.3	0.88	0.68
0.4	0.80	0.66
0.5	0.74	0.65
0.6	0.66	0.64
0.7	0.57	0.62
0.8	0.51	0.60
0.9	0.44	0.57

In Fig. 4 we make a direct comparison between simulation and experiment by plotting the respective time constants as a function of concentration. In each case the time constants have been normalized to their value at the lowest concentration. The experimentally measured time constants decrease more rapidly with initial concentration than the theoretical values, but the trends in the two sets of data are very similar. The agreement in stretching exponents β measured in our experiments and from our simulations is less impressive. In both cases the fitted exponents decrease by ~ 0.06 over the range of initial loadings available in our experiments, but the simulated exponents are systematically larger than the experimental values.

It is crucial to note that the degassing profiles examined in our experiments and our simulations are not expected to be identical. As already discussed, the experimental degassing profile arises from desorption from a large number of individual C_{60} grains. The simulation results, in contrast, describe desorption from an isolated spherical grain. The overall desorption profile from the many grains present in an experiment will not simply be the superposition of the profiles from isolated grains, since as gas desorbs from one

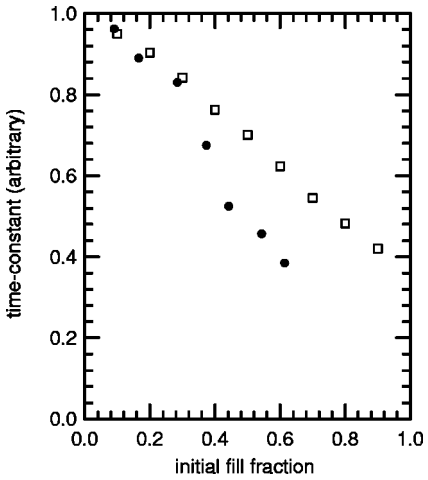

FIG. 4. A comparison between experiment and simulation. Closed circles show the experimental data and open squares the computer simulations. The time constants are obtained by stretched exponential fits to the desorption curves.

grain it may temporarily adsorb into other nearby grains before finally escaping from the overall region packed with C_{60}. It would not be possible to quantitatively model this overall process without detailed knowledge of the spatial distribution of C_{60} grains in the experiment. This type of modeling would also require specification of the molecular transport rates along boundaries and across voids between grains, which is beyond the scope of this paper.

With the caveats outlined above, we can now discuss the ability of the two diffusion models we have presented to describe our experimental observations. If multiple H_2 molecules cannot occupy a single *O* site simultaneously and the only effect of molecule-molecule interactions is to prohibit hopping into occupied *O* sites, the characteristic times and curve shapes associated with degassing are expected to be independent of initial concentration. Our experimental data is quite clearly inconsistent with this description. If H_2 diffusion is described using the dimer model of Uberuaga *et al.*, the degassing profiles of an isolated C_{60} grain are predicted to vary noticeably with initial concentration, with shorter characteristic desorption times for larger initial concentrations. This qualitative picture is completely consistent with our experimental observations from degassing of large ensembles of C_{60} grains. A comparison of this type cannot provide definitive proof that the dimer diffusion mechanism controls H_2 diffusion in C_{60}, but our experiments do provide strong support for the correctness of this mechanism.

CONCLUSION

We have experimentally measured the outgassing of H_2 from C_{60} as a function of the initial H_2 concentration within the C_{60} grains. The outgassing profiles are well described using stretched exponentials, and it is found that the time constant for outgassing decreases significantly with increasing initial H_2 concentration. To compare these observations with detailed models for H_2 diffusion in C_{60}, we used Kinetic Monte Carlo simulations of a lattice model postulated by Uberuaga *et al.* to predict the concentration dependent diffusivities of H_2 in C_{60} and subsequently used these diffusivities to numerically describe degassing of a spherical grain. The lattice model of Uberuaga *et al.* predicts that a dominant contribution to H_2 diffusion arises from the existence of metastable H_2 dimers where two H_2 molecules occupy a single interstitial site. This leads to concentration-dependent degassing profiles that are quite consistent with our experimental data. There are some quantitative discrepancies between the profiles but these are thought to occur because our theoretical model is based on an isolated C_{60} grain while the experimental results, were obtained with a large number of grains in close spatial proximity. Future work might eliminate these difficulties by examining the diffusion of H_2 within a large single crystal of C_{60}. Alternatively, techniques such as proton NMR, or quasielastic neutron scattering should be able to probe directly the diffusion mechanism under more traditional equilibrium conditions.

ACKNOWLEDGMENTS

S.A.F. acknowledges the donors of the American Chemical Society Petroleum Research Fund for partial support of this research. S.A.F. was also supported by Research Corporation Grant No. QC5999. D.D.S. was partially supported by the NSF. K.K.S. was partially supported by Jean Dreyfus Boissevain Undergraduate Scholarship for Excellence in Chemistry, sponsored by the Camille and Henry Dreyfus Foundation.

[1] A. C. Dillon, K. M. Jones, T. A. Bekkedahl, C. H. Kiang, D. S. Bethune, and M. J. Heben, Nature (London) **386**, 377 (1997).

[2] Y. Ye, C. C. Ahn, C. Withalm, B. Fultz, J. Liu, A. G. Rinzler, D. Colbert, K. A. Smith, and R. E. Smalley, Appl. Phys. Lett. **74**, 2307 (1999).

[3] K. A. Williams, B. K. Pradhan, P. C. Eklund, M. K. Kostov, and M. W. Cole, Phys. Rev. Lett. **88**, 165502 (2002).

[4] A. B. Harris and R. Sachidanandam, Phys. Rev. B **46**, 4944 (1992).

[5] M. S. Dresselhaus, G. Dresselhaus, and P. C. Eklund, *Science of Fullerenes and Carbon Nanotubes* (Academic Press, San Diego, 1996).

[6] S. A. FitzGerald, T. Yildirim, L. J. Santodonato, D. A. Neumann, J. R. D. Copley, J. J. Rush, and F. Trouw, Phys. Rev. B **60**, 6439 (1999).

[7] R. Assink, J. E. Schirber, D. A. Loy, B. Morosin, and G. Carlson, J. Mater. Res. **7**, 2136 (1992).

[8] C. P. Chen, S. Mehta, L. P. Fu, A. Petrou, F. M. Gasparini, and A. Hebard, Phys. Rev. Lett. **71**, 739 (1993).

[9] B. Morosin, J. D. Jorgensen, S. Short, G. H. Kwei, and J. E. Schirber, Phys. Rev. B **53**, 1675 (1996).

[10] I. Holleman, G. von Helden, E. H. T. Olthof, P. J. M. van Bentum,

R. Engeln, G. H. Nachtegaal, A. P. M. Kentgens, B. H. Meier, A. van der Avoird, and G. Meijer, Phys. Rev. Lett. **79**, 1138 (1997).
[11] G. E. Gadd, P. J. Evans, S. Kennedy, M. James, M. Elcombe, D. Cassidy, S. Moricca, J. Holmes, N. Webb, A. Dixon, and P. Prasad, Fullerene Sci. Technol. **7**, 1043 (1999).
[12] B. P. Uberuaga, A. F. Voter, K. K. Sieber, and D. S. Sholl, Phys. Rev. Lett. **91**, 105901 (2003).
[13] A. I. Skoulidas and D. S. Sholl, J. Phys. Chem. B **106**, 5058 (2002).
[14] D. B. Maceiras and D. S. Sholl, Langmuir **18**, 7393 (2002).
[15] W. Jost, *Diffusion in Solids, Liquids, Gases* (Academic Press, New York, 1960).
[16] S. A. FitzGerald, S. Forth, and M. Rinkoski, Phys. Rev. B **65**, 140302(R) (2002).
[17] B. Morosin, Z. Hu, J. D. Jorgensen, S. Short, J. E. Schirber, and G. H. Kwei, Phys. Rev. B **59**, 6051 (1999).
[18] J. E. Schirber, R. A. Assink, G. A. Samara, B. Morosin, and D. Loy, Phys. Rev. B **51**, 15 552 (1995).
[19] E. A. Katz, S. M. Tuladhar, D. Faiman, A. I. Shames, and S. Shtutina, Interface Sci. **9**, 331 (2001).
[20] B. Sturman, E. Podivilov, and M. Gorkunov, Phys. Rev. Lett. **91**, 176602 (2003).
[21] D. N. Theodorou, R. Q. Snurr, and A. T. Bell, in *Comprehensive Supramolecular Chemistry*, edited by G. Alberti and T. Bein (Pergamon Press, New York, 1996), Vol. 7, p. 507.
[22] J. Kärger and D. Ruthven, *Diffusion in Zeolites and Other Microporous Materials* (Wiley, New York, 1992).
[23] F. J. Keil, R. Krishna, and M. O. Coppens, Rev. Chem. Eng. **16**, 71 (2000).
[24] D. Paschek and R. Krishna, Phys. Chem. Chem. Phys. **2**, 2389 (2000).
[25] D. Paschek and R. Krishna, Phys. Chem. Chem. Phys. **3**, 3185 (2001).
[26] C. Uebing and R. Gomer, J. Chem. Phys. **100**, 7759 (1994).
[27] A. I. Skoulidas and D. S. Sholl, J. Phys. Chem. B **105**, 3151 (2001).
[28] www.comsol.com